Fluctuation-dissipation relation in a colloidal glass : frequency and aging time dependence

Bérengère Abou, François Gallet, Pascal Monceau, Noëlle Pottier

Fluctuation-dissipation relation in a colloidal glass : frequency and aging time dependence

Bérengère Abou*, François Gallet, Pascal Monceau & Noëlle Pottier
Laboratoire Matière et Systèmes Complexes (MSC), UMR CNRS 7057
Université Paris 7-Denis Diderot
2, Place Jussieu, 75251 Paris Cedex 05, France
(Dated: May 4, 2006)

We present an experimental and theoretical investigation of the Generalized Einstein Relation, a particular form of a fluctuation-dissipation relation, in an out-of-equilibrium complex fluid. Micrometer beads, used as thermometers, are immersed in an aging colloidal glass to provide both fluctuation and dissipation measurements. The fluctuation-dissipation ratio – also expressed in terms of an effective temperature – is derived as a function of frequency and aging time. We interpret the observed deviations from the Generalized Einstein Relation as directly related to the evolution of relaxation times of the glass with aging time. In accordance with our previous results, deviations are only observed in the regime where the observation time scale $1/\omega$ is of the order of a characteristic relaxation time τ of the glass, $\omega\tau \sim 1$. Our scenario is confirmed by measurements of the fluctuation-dissipation ratio in a wide range of frequencies, at long aging times.

PACS numbers: 64.70.Pf, 05.40.-a, 05.70.-a

I. MOTIVATION

During the past years, slow relaxation systems have received considerable attention in the sense that they constitute a challenge for new developments in nonequilibrium statistical mechanics theories. Such systems, which are rather common in nature, include structural glasses, polymers, colloids and granular matter. They share some characteristics called *glassy behavior*, in particular a drastic slowing down of relaxation processes when some control parameters are varied. As the characteristic relaxation times becomes longer than, or comparable to, the observation timescale, the system is said to age. The physical properties of the material depend on the waiting time, which is the time elapsed since preparation in the nonequilibrium state.

Recently, there have been serious attempts to approach and understand aging phenomena on a theoretical level. Many efforts have been devoted to apply statistical physics description – in particular, fluctuation-dissipation relations (FDR) – to out-of-equilibrium systems. At thermodynamic equilibrium, fluctuation-dissipation relations relate the response functions of the system to its autocorrelation functions, involving a single thermodynamic parameter, the equilibrium temperature. However, FDR apply only to ergodic systems at equilibrium, and are not expected to hold in out-of-equilibrium systems. The idea that a timescale dependent nonequilibrium temperature or *effective* temperature could describe the slow relaxation modes has received a lot of attention. This nonequilibrium temperature, defined from an extension of FDR, is different from the bath temperature and has been shown to display many of the properties of a thermodynamic temperature [1, 2]. Deviations from FDR have been observed in many numerical simulations [3, 4, 5, 6, 7, 8, 9, 10]. To date, there are still few experiments where FDR are studied in aging materials, such as structural glasses [11], colloidal glasses [12, 13, 14, 15, 16], spin glasses [17] and granular media [18, 19]. They show deviations from FDR as a function of waiting time and frequency. Unfortunately, no global understanding and synthesis can yet be extracted from these experimental findings.

In this paper, we measure the evolution with waiting time t_w and frequency ω of the fluctuation-dissipation ratio $\tilde{\Theta}$, leading to an effective temperature T_{eff}, in a colloidal glass of Laponite. This is achieved by simultaneously measuring the response function to an external force – using an optical tweezer – and the position fluctuations of micrometric beads embedded in the glass.

The paper is organized as follows. Sec. II is devoted to the theoretical investigation of the Generalized Einstein Relation (GER) in an out-of-equilibrium system, leading to the definition of an effective temperature. Sec. III presents the experimental procedures used to test such a GER in an aging colloidal glass: Brownian motion measurements, response to an oscillatory force and response to a step force – using optical tweezers. In Sec. IV, the fluctuation-dissipation ratio and effective temperature are derived as a function of aging time and frequency. In Sec. V, we propose a microscopic interpretation of our findings that is confirmed at long aging times. We close the paper with comparisons with other tests of FDR in the same glass and open questions.

*author to whom correspondence should be addressed : abou@ccr.jussieu.fr

II. FLUCTUATION-DISSIPATION RELATION IN AN OUT-OF-EQUILIBRIUM ENVIRONMENT

A. Frequency-dependent fluctuation-dissipation ratio $\hat{\Theta}(s)$

Let us first consider a diffusing particle of mass m evolving in a stationary medium. Its motion can be described by a generalized Langevin equation, in which $v(t) = dx/dt$ is the particle velocity, $F(t)$ the random force acting on the particle and $\gamma(t)$ a delayed friction kernel that takes into account the viscoelastic properties of the medium :

$$m\,\frac{dv}{dt} + m\int_{-\infty}^{\infty} \gamma(t-t')\,v(t')\,dt' = F(t) \qquad (1)$$

If the surrounding stationary medium is in thermal equilibrium at temperature T, a Generalized Einstein Relation – which is a specific form of a FDR with mechanical observables – can be derived :

$$s^2\langle\widehat{\Delta x^2}(s)\rangle = 2kT\,\hat{\mu}(s) \qquad (2)$$

In Eq. (2), $\langle\widehat{\Delta x^2}(s)\rangle$ is the Laplace transform of the mean-square displacement averaged over an ensemble of realizations, $\hat{\mu}(s) = 1/m\hat{\gamma}(s)$ the mobility Laplace transform, if inertia is neglected, and s is the Laplace variable.

The general situation of a particle diffusing in an out-of-equilibrium environment is much more difficult to describe. As well-known, in an aging medium, no well defined thermodynamical temperature does exist and the fluctuation-dissipation relations – in particular Eq. (2) – are no longer expected to be valid. We address the question whether the study of the diffusion and drift of the probe particle is likely to provide information about the out-of-equilibrium properties of the medium.

Experimentally, it is always possible to measure *independently* both quantities – $\langle\widehat{\Delta x^2}(s)\rangle$ and $\hat{\mu}(s)$ – during aging. One can then introduce *a priori* a fluctuation-dissipation ratio $\hat{\Theta}(s)$, parametrized by the age of the system t_w, and defined by :

$$s^2\langle\widehat{\Delta x^2}(s)\rangle = 2k\hat{\Theta}(s)\,\hat{\mu}(s) \qquad (3)$$

Eq.(3) states an out-of-equilibrium GER. This parameter $\hat{\Theta}(s)$, parametrized by the aging time t_w – analogous to the bath temperature T in a medium at equilibrium – now depends on the Laplace variable s. Note that, in an out-of-equilibrium environment where $\hat{\Theta}(s) \neq T_{\rm bath}$, the mobility of the probe particle cannot be deduced from the mean-squared displacement measurement, and *vice-versa*. As a consequence, the visco-elastic properties of the medium cannot be deduced from the single measurement of the probe thermal fluctuations and passive microrheology cannot be achieved [20].

B. Definition of the effective temperature $T_{\rm eff}(\omega)$

Since, in an out-of-equilibrium environment, even stationary, the FDR are not satisfied, one can try to rewrite them in a modified way, and thus to extend the linear response theory, with the help of a frequency-dependent effective temperature. Such a quantity, denoted as $T_{\rm eff}(\omega)$ and parametrized by the age of the system t_w, has been defined, for real ω, via an extension of the so-called Einstein relation, that relates the dissipative part of the mobility $\Re e\,\tilde{\mu}(\omega)$ and the velocity spectral density $C_{vv}(\omega) = \int_{-\infty}^{\infty}\langle v(t)v(0)\rangle\cos\omega t\,dt$, by [21, 22]:

$$C_{vv}(\omega) = kT_{\rm eff}(\omega)\,2\Re e\,\tilde{\mu}(\omega) \qquad (4)$$

It has been argued in [1, 2] that the effective temperature $T_{\rm eff}(\omega)$ defined in such a way would have a possible thermodynamic meaning, in the sense that it plays the same role as the thermodynamic temperature in systems at equilibrium (namely, it controls the direction of heat flow and acts as a criterion for thermalisation).

C. The out-of-equilibrium Generalized Einstein Relation

Here, we show how the Generalized Einstein Relation (2) is modified in an out-of-equilibrium system, making an explicit use of the fluctuation-dissipation ratio $\hat{\Theta}(s)$. This point has been developed in details in [22].

The mean-square displacement of the diffusing particle, is defined as usual by :

$$\langle\Delta x^2(t)\rangle = \big\langle[x(t) - x(t=0)]^2\big\rangle, \qquad t > 0$$

It can be deduced from the velocity correlation function *via* a double integration over time :

$$\langle\Delta x^2(t)\rangle = 2\int_0^t dt_1\int_0^{t_1} dt_2\,\big\langle v(t_1)v(t_2)\big\rangle$$

By Laplace transforming the above expression of $\langle\Delta x^2(t)\rangle$, one gets :

$$s^2\,\langle\widehat{\Delta x^2}(s)\rangle = 2\,\big\langle\hat{v}(s)v(t=0)\big\rangle$$

The quantity $\big\langle\hat{v}(s)v(t=0)\big\rangle$ can be obtained by Laplace transforming the expression of $\langle v(t)v(0))\rangle$ as a cosine Fourier transform of $C_{vv}(\omega)$:

$$\big\langle\hat{v}(s)v(0)\big\rangle = \int_{-\infty}^{\infty}\frac{d\omega}{2\pi}\,\frac{s}{s^2+\omega^2}\,C_{vv}(\omega)$$

Introducing the expression (4) of $C_{vv}(\omega)$ in the above equation, one gets :

$$s^2\,\langle\widehat{\Delta x^2}(s)\rangle = 2\int_{-\infty}^{\infty}\frac{d\omega}{\pi}\,\frac{s}{s^2+\omega^2}\,kT_{\rm eff}(\omega)\,2\Re e\,\tilde{\mu}(\omega).$$

Using standard contour integration, this takes the form :

$$s^2 \langle \widehat{\Delta x^2}(s) \rangle = 2k\hat{\Theta}(s)\,\hat{\mu}(s) \tag{5}$$

with the following relationship between $\tilde{\Theta}(\omega)$ and $T_{\rm eff}(\omega)$:

$$T_{\rm eff}(\omega)\,\Re e\tilde{\mu}(\omega) = \Re e\big[\tilde{\mu}(\omega)\tilde{\Theta}(\omega)\big] \tag{6}$$

where $\hat{\mu}(s) = \tilde{\mu}(\omega = is)$ and $\hat{\Theta}(s) = \tilde{\Theta}(\omega = is)$.

Equations (5) and (6) are the extension to an out-of-equilibrium medium of the Generalized Einstein Relation $s^2 \langle \widehat{\Delta x^2}(s) \rangle = 2kT\,\hat{\mu}(s)$, valid for a medium in equilibrium. As can be seen in Eq. (5), independent measurements of the particle mean-square displacement and frequency-dependent mobility in an aging medium give access, once $\langle \widehat{\Delta x^2}(s) \rangle$ and $\hat{\mu}(s) = \tilde{\mu}(\omega = is)$ are determined, to the fluctuation-dissipation ratio $\hat{\Theta}(s)$. Eq. (6) then allows to derive an effective temperature $T_{\rm eff}(\omega)$ from the experimentally measurable function $\tilde{\Theta}(\omega) = \hat{\Theta}(s = -i\omega)$.

III. EXPERIMENTAL PROCEDURES

A. Samples preparation

The experiments were performed on Laponite RD, a synthetic clay manufactured by Laporte Industry. The particles of Laponite are colloidal disks of 25 nm diameter and 1 nm thickness, with a negative surface charge on both faces [23]. The clay powder was mixed in ultrapure water, and the pH value of the suspensions fixed to pH = 10 by addition of NaOH, providing chemically stable particles [24]. The suspension was stirred vigorously during 15 minutes and then filtered through a Millipore Millex - AA 0.8 μm filter unit. This procedure allows us to prepare a reproducible initial liquid state. The aging time $t_w = 0$ of the suspension is defined as the moment it passes through the filter.

These aqueous suspensions form glasses for low volume fraction in particles [25]. Starting from a viscous "liquid" state right after preparation, the suspension becomes more and more viscoelastic with time. Since the physical properties of the suspension depend on the time t_w elapsed since preparation, the sample is said to age. Aging can be seen through the evolution of both the viscoelastic properties and of the colloidal disks diffusion [26, 27]. Laponite suspensions age on timescales that depend on the particles concentration. We are thus able to monitor the aging timescales of the glass by adjusting this concentration. With a volume fraction of 2.3% wt, the glass evolves over several hours, slowly enough to allow quasi-simultaneous measurements of the fluctuation and dissipation properties, within a few minutes, without significative aging of the sample. These two successive measurements are thus considered to be performed at the same waiting time t_w.

The experiments were carried out in a square chamber – 20×20 mm^2 – made of a microscope plate and a coverslip separated by a thin spacer (0.1 mm thickness). The beads are suspended in the glass right after its preparation. The chamber is then filled with the suspension, sealed with vacuum grease and mounted on a piezoelectric stage on the plate of an optical microscope. The probes are latex and silica beads, in very low concentration (respectively 10^{-4}% and 4.10^{-4}% in volume). Latex beads ($1.0 \pm 0.1\mu$m in diameter, Polysciences, Inc.), were preferentially used for fluctuation measurements : since they do not deposit during the experiment, their random motion is not perturbated by the chamber walls. Silica beads ($2.1 \pm 0.1\mu$m in diameter, Bangs Lab Inc.) were used for dissipation measurements, because they are more efficiently trapped by the optical tweezers. The diameters of the two kinds of probes are close to each other, thus the comparison between the results of the fluctuation and dissipation measurements, once rescaled to the same diameter, is meaningful.

B. Thermal fluctuations of the beads

At a given aging time t_w, we record the fluctuating motion of 1 μm latex beads during 8 s, with a fast CCD camera sampling at 250 Hz (Fastcam-PHOTRON LTD). A digital image analysis allows to track the bead positions $x(t)$ and $y(t)$ close to the focus plane of the microscope objective. For each bead, we calculate the time-averaged mean-square displacement $\langle \Delta r^2(t) \rangle_{t'} = \langle [x(t'+t) - x(t')]^2 + [y(t'+t) - y(t')]^2 \rangle_{t'} = 2\langle \Delta x^2(t) \rangle_{t'}$. To preserve a good statistics, we keep the data of $\langle \Delta r^2(t) \rangle_{t'}$ in the range $0.004 < t < 1$ s. The glass remains in a quasi-stationary state during the recording, which takes a short time compared to the aging timescale. The quantity $\langle \Delta r^2(t) \rangle_{t'}$, averaged over several beads and realizations, can thus be identified to the ensemble-averaged mean-square displacement.

C. Dissipative response to an oscillatory force

We describe now the measurement of the mobility $\tilde{\mu}(\omega)$, at a given frequency ω, for various aging times t_w. This measurement is performed immediately after the Brownian motion recording, at the same aging time t_w. Since the aging Laponite suspension is a viscoelastic fluid, the bead mobility $\tilde{\mu}(\omega) = |\tilde{\mu}(\omega)| e^{i\varphi(\omega)}$ is a complex number. We thus need to measure the phase and modulus of the tracer mobility. We use an optical tweezer to trap a 2.1 μm silica bead immersed in the glass. Trapping is achieved by focusing a powerful infrared laser beam (Nd YAG, Spectra-Physics, $P_{max} = 600$ mW) through a microscope objective of large numerical aperture [28]. The trapping force F on a small dielectric object like a silica bead is proportional to the intensity gradient in the focusing region. It depends on the distance x

of the center of the trapped object from the center of the trap, according to $F(x) = -kx(1 + \epsilon|x|)$. The corrective factor ϵ is introduced to take into account the non-harmonicity of the trapping potential. The trap stiffness k and the factor ϵ are determined from an independent calibration. Once the bead is trapped, we make the experimental chamber oscillate by monitoring the displacement $x_p \exp(i\omega t)$ of a piezoelectric stage. Neglecting in a first step the viscoelastic fluid inertia, the fluid displacement x_f in the bead vicinity is taken equal to the piezolectric stage displacement x_p. The validity of this assumption is discussed in subsection III E. Due to the relative bead/fluid motion, the viscoelastic fluid exerts a sinusoidal force $F' \exp(i\omega t)$ on the bead. We record with the fast camera the bead movement, and measure by conventional image analysis its displacement $x \exp(i\omega t)$ from the trap center. Notice that x is a complex number which includes a phase shift due to the fluid viscoelasticity. At a given frequency ω, the force amplitude $F'(\omega)$ is given by $\tilde{F}'(\omega) = \tilde{v}(\omega)/\tilde{\mu}(\omega)$, where $\tilde{v}(\omega) = i\omega(x_f - x) = i\omega(x_p - x)$ is the relative glass/bead velocity, and $\tilde{\mu}(\omega)$ the Fourier transform of the bead mobility. In our range of experimental frequencies ($0.5 \leq f \leq 10$ Hz), the bead inertia is negligible, so that we can simply use the relation $F + F' = 0$ to calculate $|\tilde{\mu}(\omega)|$ and $\varphi(\omega)$. Notice that the motion of the piezoelectric stage is numerically controlled by a sequence of successive sinusoidal signals at five different frequencies $\{0.5, 1, 2, 5, 10\}$ Hz. The same program synchronously generates a sequence of pulses to trigger the image acquisition, so that the phase shift between the force and the bead movement can be accurately measured.

D. Dissipative response to a step force

Another method that we used to measure the bead mobility $\hat{\mu}(s)$ consists in submitting the bead to a step of force and recording its position $x(t)$ during its relaxation in the trap. This is achieved by instantaneously displacing the piezoelectric stage at $t = 0$ by an amount x_{0p} of the order of one micrometer. Neglecting the fluid inertia (see subsection III E for the validity domain), the motions x_{0f} and x_{0p} of the fluid and the stage respectively are identical, and the step force amplitude at $t = 0$ is $F(x_{0p})$. During the relaxation, we record with the fast camera the bead position $x(t)$, from which we calculate the instantaneous force $F[x(t)]$ exterted on the bead. Taking the Laplace transform of Eq. (1) with the external force $F(x)$, and with negligible bead inertia, the bead mobility can be derived from :

$$\hat{\mu}(s) = \frac{s\hat{x}(s) - x_{0p}}{\hat{F}(s)} \tag{7}$$

This method presents the advantage to give the value of $\hat{\mu}(s)$ in a continuous frequency range, which is in principle determined by the camera sampling frequency and the recording time. This range is typically $0.2 < s < 250$ s^{-1}. However, we show in next subsection that this frequency range must be narrowed, in order to remain in the validity domain of Eq. (7).

Also, this procedure cannot be used at the early stage of aging time t_w, when the typical relaxation time of the bead is too small to be resolved by the fast camera. The minimum viscosity modulus of the glass, at which the response to a step force may be recorded, is then about 10^{-1} Pa.s.

We recorded the bead response to a step force immediately after measuring the response to an oscillatory force, and after the mean square displacement recording. In these conditions the aging time t_w can be taken as the same for the three experiments.

E. Data processing

For both the mean-square displacement experiments and the active microrheology experiments, we used a conventional image processing software (IMAQ vision builder from National Instruments) to determine the bead position from the numerical recording of the bead images. The accuracy on the bead position was about 10 nm, for typical motions comparable to the bead radius, in the micrometer range.

We calculated the Laplace transforms by numerical integration of the discrete sampled data. We used both home made codes and a routine of the NAG libraries implementing the Gill–Miller method. As a matter of fact, the tests we performed show that the results are independent of the chosen method, within the reliability range of the Laplace transforms. Calling δt the sampling time and N the total number of points recorded during a given experiment, a numerical Laplace transform can be reliable only over a finite frequency range, upper bounded by half the sampling frequency $1/(2\delta t)$, and lower bounded by twice the inverse of the total time of the experiment $2/[(N-1)\delta t]$. Practically, this reliability range is the largest possible one, and we were led to restrict it by taking in account other uncertainties linked to the behavior of the physical quantities we measured. In the step force experiment, the too small value of the sampling frequency, added to the residual noise in the bead position, do not allow to trust the Laplace transform calculated at the highest frequencies, especially when the relaxation of the bead is too fast. Thus, we decided to discard the frequencies above 125 s^{-1}, even when the sampling frequency was as high as 500 s^{-1}. Moreover, the troncature of the integral can induce systematic errors in the Laplace transform which must be carefully evaluated. Let us recall that the effect of the truncature is larger at low frequencies particularly when the physical quantity is an increasing function of time (which is the case for $\langle \Delta r^2(t) \rangle$). Anyway, in each case, we evaluated an upper bound of the truncature effect and included it in our error bars.

The relative statistical uncertainties on $\hat{\mu}(s)$ in the step force experiments were calculated in the following way: We first evaluated the effect of the mean noise amplitude affecting $F(t)$ and $x(t)$ on their Laplace transforms; we added also a term associated with the uncertainty on the initial position x_{0p}. At last, we included the systematic errors due to the above mentioned truncature effects.

Another important issue is the possible influence of the fluid inertia in active microrheology measurements. Indeed, when the experimental chamber is shaked by the piezoelectric stage, the motion x_f of the viscoelastic fluid filling the chamber may not exactly follow the plate motion x_p, especially at high frequency. The relevant dimensionless parameter of the problem is the relative difference $\xi = \frac{x_f - x_p}{x_p}$, which we estimated as $\xi = s\hat{\mu}(s)M$, where $M = 3\pi/2\rho R d^2$, $d \simeq 100$ μm is the thickness of the experimental chamber, and $R = 1.05\,\mu$m is the bead radius. This value M is of the order of the mass of the fraction of fluid in relative motion with the bead. In our geometry, an upper bound for M is 5.10^{-11} kg. Consequently, the fluid inertia can be neglected as soon as $s\hat{\mu}(s) \ll 2.10^4$ μm.s^{-1}.pN^{-1}. This gives an upper limit of confidence for the values of $\hat{\mu}(s)$ retrieved by this method.

We also performed an independent check of our microrheological techniques : we tested the oscillatory and step force methods on Maxwellian fluids (CPyCl/NaSal (100mM/60mM) in water [29]) having given viscoelastic properties, close to the ones of our colloidal glasses at large t_w. We verified the agreement between the measured values of $\tilde{\mu}(\omega)$ by the oscillatory force method and of $\hat{\mu}(s)$ by the step force method.

IV. RESULTS

A. Brownian motion of beads in the glass

Figure 1 shows the mean-square displacement of latex beads immersed in the colloidal glass, as a function of time t, for various aging times t_w. At $t_w = 0$, we observe a nearly diffusive behavior of the tracer beads, characterized by a linear dependency of the mean-square displacement with time. Upon increasing on t_w, the tracer motion becomes sub-diffusive.

B. Mobility from oscillatory force

Figure 2 shows the frequency and aging time dependence of the complex mobility modulus $|\tilde{\mu}(\omega)|$ and phase $\varphi(\omega)$ measured when applying an oscillatory external force at successive frequencies $\{0.5, 1, 2, 5, 10\}$ Hz. The mobility modulus $|\tilde{\mu}(\omega)|$ of the bead was found to decrease with aging time t_w as shown in Fig. 2(a). This corresponds to the increase in the visco-elastic modulus of the glass. Fig. 2(b) represents the evolution of the phase shift $\varphi(\omega)$ as a function of t_w. The phase φ decreases

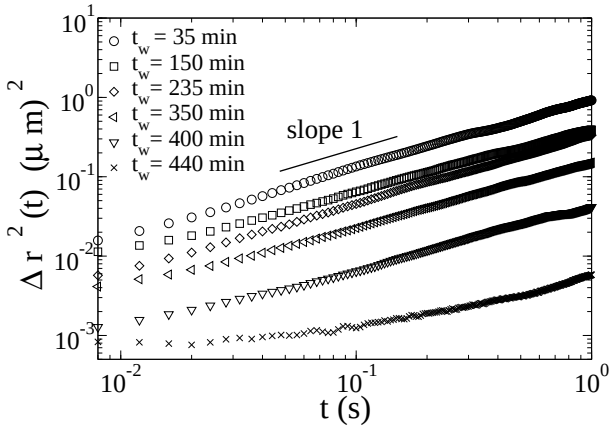

FIG. 1: Mean-square displacement of 1 μm latex beads immersed in the glass, as a function of time. The curves correspond to different aging times $t_w = 35, 150, 235, 350, 400$ and 440 minutes from top to bottom, measured for one realization. The fluctuating motion is purely diffusive at short t_w, and becomes sub-diffusive as the glass ages.

with t_w and in a first-order approximation, remains independent of the frequency. Figure 2(c) shows the same $|\tilde{\mu}(\omega)|$ data, plotted as a function of the frequency ω, for different aging times t_w. The mobility modulus $|\tilde{\mu}(\omega)|$ is well fitted by a power law $|\tilde{\mu}(\omega)| = \mu_0(\omega/\omega_0)^\beta$ in the experimental frequency range corresponding to one and half decade. Here, ω_0 is an arbitrary reference frequency set to $\omega_0 = 1$ rad.s^{-1} for convenience. Starting from about zero at low aging times, the exponent β increases with t_w. Since $|\tilde{\mu}(\omega)|$ exhibits a power-law behavior, the dependence of $\varphi(t_w)$ must be related to β by $\varphi(t_w) = -\beta(t_w)\pi/2$. This is a consequence of the Kramers-Kronig relations, and ensures that $\hat{\mu}(s)$ is a real number. In Fig. 2(b), we plot the quantity $-\beta(t_w)\pi/2$ (full circles), which is in good agreement with the experimental data $\varphi(t_w)$.

C. Scaling of the aging dynamics

Fig. 3(a) shows the evolution of the viscosity modulus with waiting time for a set of six different realizations. The complex mobility of a Laponite suspension at 2.3% wt was measured by applying an oscillatory force on a silica bead in the linear regime. The complex viscosity modulus $|\tilde{\eta}(\omega)|$ was estimated from the complex mobility modulus $|\tilde{\mu}(\omega)|$ assuming that the Stokes relation $\tilde{\mu}(\omega) = \frac{1}{6\pi R\tilde{\eta}(\omega)}$ remains valid in the complex fluid. Starting from a value close to the water viscosity 10^{-3} Pa.s, the viscosity modulus of the glass is shown to increase by 3 orders of magnitude over about $200-400$ minutes. In such suspensions, the aging dynamics is known to drastically depend on the particle concentration. In a suspension at 2.5% wt, a three orders of magnitude increase of the complex viscosity modulus is reached after 50 minutes, while in a 3.5% wt suspension, the same

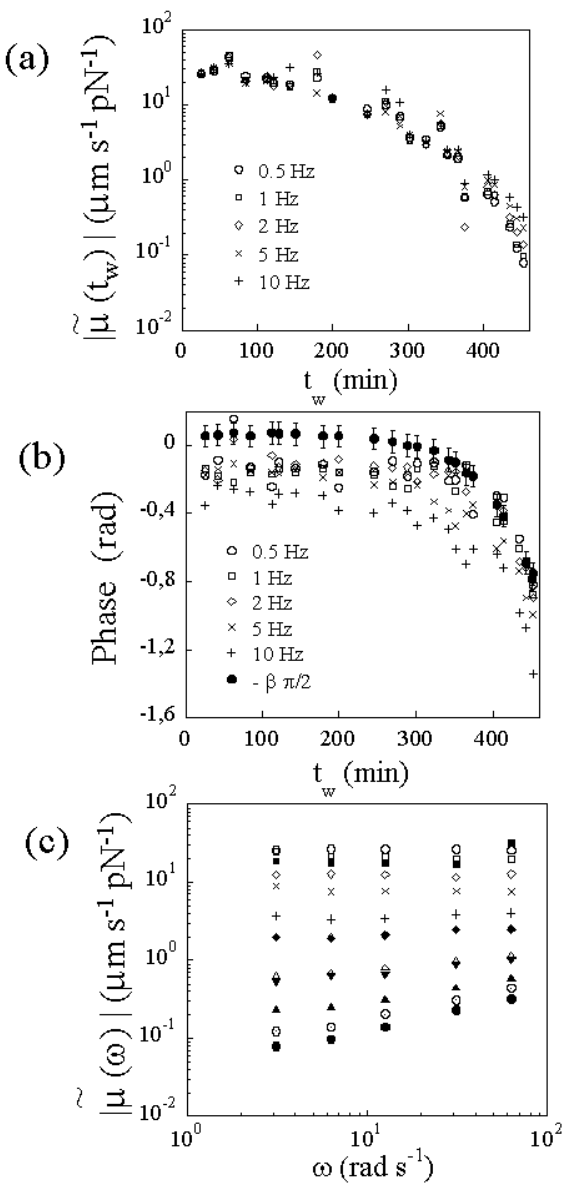

FIG. 2: Modulus (a) and phase (b) of the complex mobility $\tilde{\mu}(\omega) = |\tilde{\mu}(\omega)|e^{i\varphi(\omega)}$ of the bead as a function of t_w, for various frequencies of the applied force; (c) mobility modulus versus ω for various t_w; from top to bottom, t_w varies from 20 to 450 min, for this realization. At low t_w, $|\tilde{\mu}(\omega)|$ is nearly independent of ω. Upon increasing t_w, the modulus is well fitted by a power-law $|\tilde{\mu}(\omega)| = \mu_0(\omega/\omega_0)^\beta$ with $\omega_0 = 1$ rad.s^{-1} and β only depending on t_w. The full circles in (b) correspond to $\varphi(t_w) = -\beta(t_w)\pi/2$.

increase is reached after 10 minutes [27]. We therefore assume that the differences in the aging dynamics shown in Fig. 3(a) are due to slight concentration differences in Laponite particles from one experiment to the other. In Fig. 3(b), the different curves are rescaled in time by considering that the same glass formation process is reached after an increase of 3 orders of magnitude in the viscosity. The aging time is then linearly stretched to

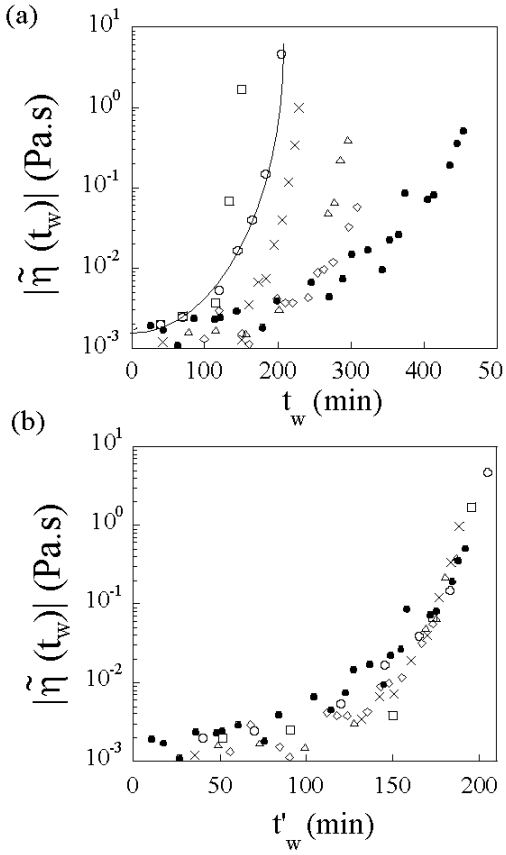

FIG. 3: (a): Viscosity modulus of the glass as a function of aging time, for six different realizations. The viscosity modulus was measured by applying an oscillatory force at a frequency $f = 1$ Hz on a silica bead in the linear regime; (b): Scaling of the complex viscosity modulus. The aging time is linearly stretched $t_w \to t'_w = \alpha t_w$ to make the viscosities roughly coincide for all experiments, choosing a particular realization as a reference.

make the viscosities roughly coincide for all experiments, choosing a particular realization as a reference. With this scaling, we are now able to average over different realizations. From now on, when possible, the aging times of the different realizations are rescaled by using this scaling.

D. Effective Temperature derived from oscillatory measurements

The fluctuation-dissipation ratio $\hat{\Theta}(s)$ is now derived from the oscillatory and Brownian motion measurements. The selected range $s \in [3; 60]$ s^{-1} corresponds to the experimental frequencies range $f \in [0.5; 10]$ Hz.

From the oscillatory measurements, the variations of $\tilde{\mu}(\omega)$ are well represented by the analytical form $\tilde{\mu}(\omega) = \mu_0(\omega/\omega_0)^\beta \exp(-i\beta\pi/2)$. The Laplace transform $\hat{\mu}(s) = \tilde{\mu}(\omega = is) = \mu_0(s/s_0)^\beta$ is then derived by analytical continuation. Again, s_0 is an arbitrary reference frequency set to $s_0 = 1$ s^{-1}.

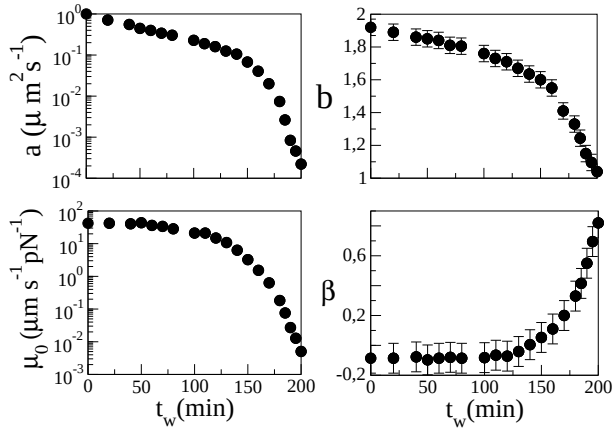

FIG. 4: Top: Evolution of the Brownian motion parameters a and b as a function of aging time, where $\langle\widehat{\Delta r^2}(s)\rangle = a(s/s_0)^{-b}$, with $s_0 = 1$ s^{-1}; Bottom : Evolution of the mobility parameters μ_0 and β as a function of aging time, where $\tilde{\mu}(\omega) = \mu_0(\omega/\omega_0)^{\beta}\exp(-i\beta\pi/2)$, with $\omega_0 = 1$ rad.s^{-1}. The results have been averaged over six realizations rescaled in aging time.

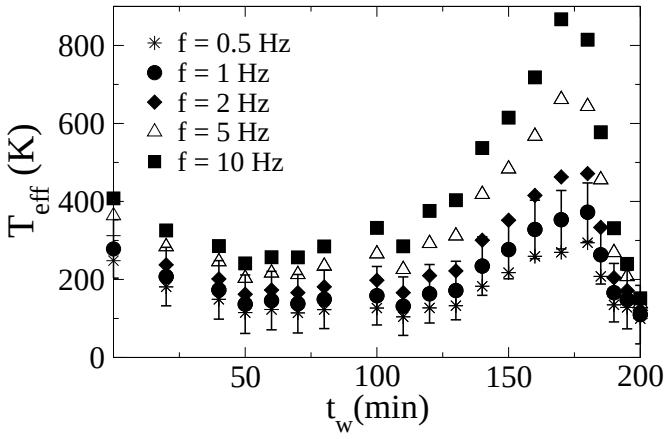

FIG. 5: Effective temperature $T_{\rm eff}$ of the colloidal glass as a function of aging time t_w, measured at different frequencies. The results have been averaged over six realizations. Upon increase on t_w, $T_{\rm eff}$ increases up to about 2-3 times the bath temperature and then decreases back.

As can be seen in Fig. 1, $\Delta r^2(t)$ can be adjusted by a power-law in the range $t \in [0.015; 0.3]$ s. As a consequence, in the corresponding range $s \in [3; 60]$ s^{-1}, the Laplace transform of the mean-square displacement is well described by a power-law $\langle\widehat{\Delta r^2}(s)\rangle = a(s/s_0)^{-b}$. Fig. 4 shows the evolution of the parameters a, b, μ_0 and β with aging time t_w, averaged over a set of six different realizations using the time rescaling described in section IV C.

The exponent b decreases from about 1.9 ± 0.05 to 1 ± 0.05 while the exponent β increases from about zero at low aging times to 0.82 ± 0.1 at the end of experiment. This is consistent with the evolution of the glass from viscous to elastic behavior.

Bringing together our data for $\langle\widehat{\Delta r^2}(s)\rangle$ and $\hat{\mu}(s)$, and using the modified Generalized Einstein Relation (5), the function $\hat{\Theta}(s)$, parametrized by t_w, is adjusted by :

$$\hat{\Theta}(s) = \frac{a}{4k\mu_0}(s/s_0)^{2-b-\beta}$$

in the range $s \in [3, 60]$ s^{-1}.

After analytical continuation of $\tilde{\Theta}(\omega) = \hat{\Theta}(s = -i\omega)$, we derive the effective temperature $T_{\rm eff}(\omega)$, at a given t_w, from :

$$T_{\rm eff}(\omega) = \frac{a}{4k\mu_0}\frac{\cos[(b-2)\pi/2]}{\cos(\beta\pi/2)}(\omega/\omega_0)^{2-b-\beta} \qquad (8)$$

in the range $\omega \in [3; 60]$ rad.s^{-1}.

The dependence of the effective temperature $T_{\rm eff}$ with aging time t_w, at different frequencies, is shown in Fig. 5. The results have been averaged over six realizations. At the earliest t_w, the effective temperature is close to the bath temperature $T_{\rm bath} = 300$ K. Upon increase on t_w, $T_{\rm eff}$ increases up to 2-3 times the bath temperature and then decreases back upon further increase on t_w. Such a behavior – an increase of $T_{\rm eff}$ followed by a decrease – was observed for the first time in a colloidal glassy system in [14], where a realistic explanation of this non-monotonic behavior was proposed. In the range $\omega \in [3; 60]$ rad. s^{-1}, $T_{\rm eff}$ increases with frequency for all aging times as seen in Fig. 5.

Note that in a system at equilibrium, $\hat{\Theta}(s)$ would be independent on the frequency s. We should have $\frac{a}{4k\mu_0} = T_{\rm bath}$ and $2-b-\beta = 0$, which leads to $\hat{\Theta}(s) = T_{\rm bath}$ and $T_{\rm eff}(\omega) = T_{\rm bath}$. This is not the case here for the aging colloidal glass.

E. Fluctuation-dissipation ratio derived from step force measurements

The fluctuation-dissipation ratio $\hat{\Theta}(s)$ is derived from step force measurements of the mobility and Brownian motion measurements. Figure 6 shows the results for the bead mobility $\hat{\mu}(s)$, at long aging times t_w. The experimental procedure for the step force measurements – described in section III D – cannot be used at the earliest aging times t_w, when the typical relaxation time of the bead after a step force is smaller than the sampling rate of the fast camera. Nevertheless, it allows us to extend to lower frequencies the range s of the mobility measurements $\hat{\mu}(s)$.

We compared first the mobilities $\hat{\mu}(s)$ independently obtained from step and oscillatory measurements. As shown in Fig. 6, the agreement between the experimental values of mobilities is good in the common range. Nevertheless, for the highest values of s, the step measurements of $\hat{\mu}(s)$ show systematic deviations from the power-law analysis of section IV D.

Besides, $\langle\widehat{\Delta r^2}(s)\rangle$ is numerically calculated from

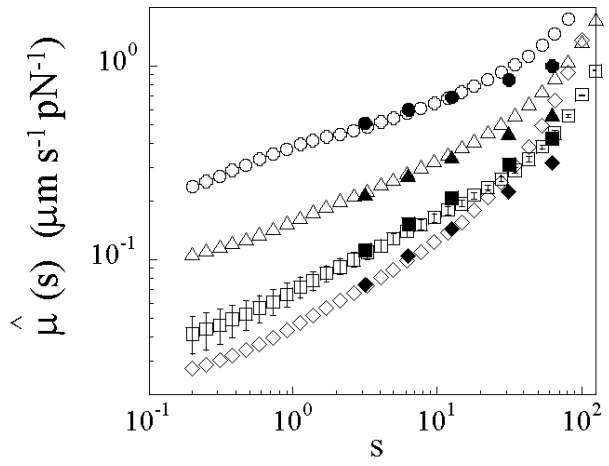

FIG. 6: Comparison between $\hat{\mu}(s)$ obtained from oscillatory external force (black symbols) and $\hat{\mu}(s)$ obtained from step force (open symbols), at different aging times $t_w = 175, 183, 187$ and 191 minutes (top to bottom), for one realization rescaled in aging time. The agreement between the two sets of values is excellent at lowest s.

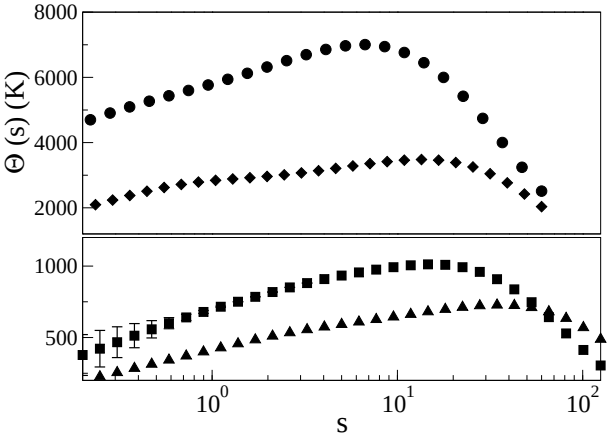

FIG. 7: Fluctuation-dissipation ratio $\hat{\Theta}(s)$ for different long aging times $t_w = 182, 190, 195$ and 201 minutes, from bottom to top, for one realization rescaled in aging time.

$\langle\widehat{\Delta r^2}(t)\rangle$ in the whole accessible range of $s \in [0.2; 125]$ s^{-1}.

From $\langle\widehat{\Delta r^2}(s)\rangle$ and $\hat{\mu}(s)$ in the reliable range $s \in [0.2; 125]$ s^{-1}, we derive the fluctuation-dissipation ratio $\hat{\Theta}(s)$, as shown in Fig. 7. The frequency dependence at lowest s is consistent with the power-law analysis of section IV D. The fluctuation-dissipation ratio $\hat{\Theta}(s)$ exhibits a maximum value at $s = s_{max,t_w}$. In Fig. 7, s_{max,t_w} is shown to decrease as t_w increases.

V. DISCUSSION AND CONCLUSION

The key results of this paper are the dependence of the fluctuation-dissipation ratio and effective temperature on aging time and frequency (Fig. 5 and 7). As previously reported in [14], the unusual dependence of $T_{\rm eff}$ on t_w can be explained through the evolution of the relaxation times of the glass with aging time. In colloidal glasses, dynamic light scattering and diffusive wave spectroscopy experiments provide the opportunity to probe the relaxation times associated to the colloidal particles diffusion [26, 31, 32]. The resulting distribution function of relaxation times $P(\tau)$, centered around two characteristic relaxation times $\tau_{\rm fast}$ and $\tau_{\rm slow}$, is schemed in Fig. 8. Upon increasing t_w, part of the modes distribution function, centered around $\tau_{\rm slow}$, shifts to larger times, while the mode at $\tau_{fast} \sim 0.1$ ms remains unchanged.

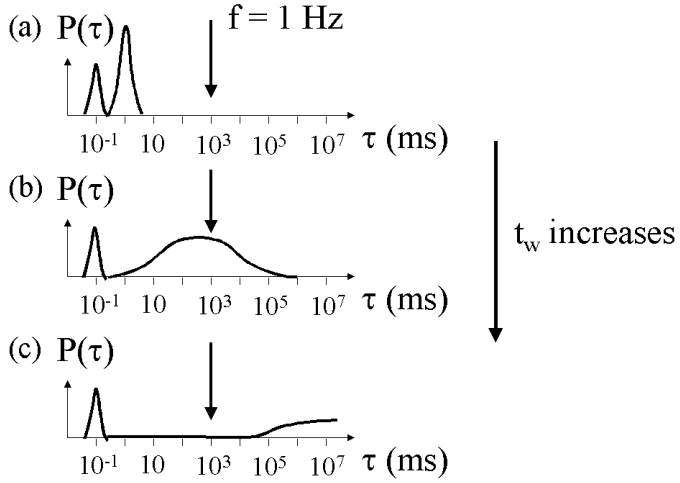

FIG. 8: Scheme of the distribution function of relaxation times $P(\tau)$ in the glass of Laponite (typically 2.5% wt) at different aging times t_w. Upon increasing t_w, part of the modes distribution, centered around $\tau_{\rm slow}$, shifts towards larger times, while the mode at $\tau_{\rm fast} \sim 0.1$ ms remains unchanged. The arrow represents the measurements timescale $1/f$.

We propose the following scenario to explain the dependence of the effective temperature on the aging time. When probing the colloidal glass at a typical frequency $f = 1$ Hz, three situations successively occur upon increasing t_w. At the earliest t_w, the relaxation times of the glass are small compared to the observation time scale $\tau_{\rm fast,slow} \ll 1/f$ and do not play any role on this observation time. The glass is "*at equilibrium*". In this experiment, the bead is small enough to be sensitive to molecular fluctuations. This ensures that it can thermalize with the bath when the relaxation times of the glass do not play any role on the observation time scale. In this case, the reading of the bead thermometer reduces to $T_{\rm bath}$. Upon increase on t_w, relaxation modes of the order of the observation time scale $\tau_{\rm slow} \sim 1/f$

appear in the glass as seen in Fig. 8 b. On this observation timescale $1/f$, the system is *out-of-equilibrium* : the measured temperature becomes different from the bath temperature. Deviations from the Generalized Einstein Relation are thus observed. Finally, for very long t_w, the first situation is recovered. The slow and fast relaxation processes of the glass do not play any role at the experimental observation timescale because $\tau_{\rm slow} \gg 1/f$ and $\tau_{\rm fast} \ll 1/f$. The bead thermometer, only sensitive to the fast relaxation processes at the molecular scale, again thermalizes with the bath. The measured temperature is then expected to reduce back to $T_{\rm bath}$. Finally, in this scenario, deviations are only observed in the regime where the observation time scale is of the order of a characteristic relaxation time of the glass, $\omega\tau \sim 1$ [14].

These different situations are clearly identified in Fig. 5. However the experimental set-up does not allow to measure $T_{\rm eff}$ at longer t_w. Indeed, beyond $t_w = 200$ minutes, the mobility modulus becomes smaller than 10^{-2} m $\rm s^{-1}pN^{-1}$. In this range, the optical tweezer is not powerful enough to induce a detectable motion of the bead.

As described in [2, 33], the temperature of an object is measured by coupling it to a thermometer during a sufficiently long time interval such that all heat exchanges between thermometer and system take place and the whole system equilibrates. In [2], the authors consider an oscillator of characteristic frequency ω_0 as a thermometer, weakly coupled to a glassy system in which a regime with small flows of energy exists. The glass exhibits two time correlation scales, a fast one and a slow one, such that: $R_{ST}(t-t_w) = \frac{1}{kT}\partial_{t_w} C_{ST}(t-t_w)$ is satisfied at short times $t - t_w \ll t_w$ and $R_{AG}(t_w/t) = \frac{1}{kT^*}\partial_{t_w} C_{AG}(t_w/t)$ is satisfied if $t_w/t = O(1)$. R_{ST} and C_{ST} (or R_{AG} and C_{AG}) are respectively the stationary or aging parts of the response and correlation functions. T is the bath temperature and T^* is the temperature associated to FDR when $t_w/t = O(1)$.
If ω_0 is high enough so that the thermometer evaluates the fast relaxation and quasiequilibrium is achieved on the time scale $1/\omega_0$, its asymptotic internal energy density reads $E_{\rm THERM} = kT$. The reading of the thermometer is the bath temperature T. If ω_0 is very low, the thermometer examines the system in its long time scales behavior and one finds $E_{\rm THERM} = kT^*$, where T^* is identified as the temperature of the system on this observation time. Any small but macroscopic thermometer, weakly coupled to the system, is shown to play the same role as the above considered oscillator. The role of ω_0 is then played by the inverse of the typical response time of the thermometer.

In our experiments, the bead plays the role of a thermometer which characteristic frequency ω_0 is set to the probing frequency ω. Indeed, the bead inertia is negligible below $\omega_{\rm inertia} = 10^{12}$ rad.$\rm s^{-1}$ for the highest value of the fluid viscosity ($\simeq$ 10 Pa.s). Experimentally, the observation time scale $1/\omega$ is much higher than the typical response time of the bead thermometer $1/\omega_{\rm inertia}$. As a result, the response time of the bead is set to the observation time scale $1/\omega$. It follows that by changing this observation time scale, the thermometer can explore or be sensitive to, different relaxation time scales of the glass (see Fig. 8).

In our scenario, the aging time at which the fluctuation-dissipation ratio $\hat{\Theta}(s_0, t_w)$ exhibits a maximum value is expected to decrease with the probing frequency s_0. In an equivalent point of view, the value of s at which the fluctuation-dissipation ratio $\hat{\Theta}(s, t_{w0})$ exhibits a maximum value is expected to decrease with aging time t_{w0}. This behavior is identified at long aging times in Fig. 7. The maximum value of $\hat{\Theta}(s)$ is shown to decrease as the aging time increases. Our scenario is thus confirmed in the long aging time limit. In Fig. 5, one can detect a very slight shift of the maximum value of $T_{\rm eff}(t_w)$ towards low aging times upon increase of the frequency, which again is consistent with our interpretation.

In models and simulations – where the characteristic relaxation time of the system is set to the waiting time – deviations are observed when the characteristic observation time $1/\omega$ is of the same order or greater than the aging time t_w. Experimentally, deviations are observed in the other regime when $1/\omega \ll t_w$. In our sense, this discrepancy arises because the aging time t_w is not the only relevant parameter to describe aging, and that microscopic processes, characterized by the distribution of relaxation times in the system, must be considered. In our experiments, deviations are observed when $\omega\tau \sim 1$. This suggests that, besides the waiting time t_w, the distribution of relaxation times must be included in models to get an accurate description of aging. This has been recently achieved in [34], where the existence of a resonant peak for a nonequilibrium temperature has been evidenced.

In the past, FDR have been experimentally investigated in the *same colloidal glass* with electrical and rheological measurements [13]. In the dielectric measurements, the effective temperature is found to decrease with t_w and ω, and reaches the bath temperature at high frequency and aging times. In the rheological measurements, no deviation from FDR could be detected. More recently, FDR, in the form of a Generalized Stokes-Einstein relation, has been investigated by combining dynamic light scattering and rheological measurements [15]. The authors assume that the bulk stress relaxation probed by a rheometer is the same as the local stress relaxation affecting the probe particles. The effective temperature is shown to increase with frequency and aging time in the range $t_w \in [82; 135]$ min and $\omega \in [20; 100]$ rad. $\rm s^{-1}$ for a 3% wt suspension. The authors propose the existence of two regimes: $\omega\tau \ll 1$ leading to $T_{\rm bath}$ and $\omega\tau \gg 1$ leading to $T_{\rm eff}$, which is not consistent with our interpretation despite the authors claim. Another group has investigated the deviations from FDR, by performing a test of the Stokes-Einstein relation, using optical tweezers [16]. Surprisingly, they found that no deviation could be detected in the aging colloidal glass over a wide range of frequencies $f \in [1.2; 12000]$ Hz. Besides, our

experimental findings are fully supported by microscopic processes probed in light scattering experiments.

In conclusion, this work provides an experimental and theoretical investigation of the Generalized Einstein Relation in an aging colloidal glass. We interpret the observed deviations from GER as directly related to the evolution of the relaxation times of the glass. Deviations are observed in the regime $\omega\tau \sim 1$, in agreement with the evolution of relaxation times of the glass during aging. This interpretation is confirmed at long aging times.

At this stage, whether these experimental investigations with the same observables, in the same colloidal glass, are in contradiction still remains an open question [14, 15, 16]. Furthermore, the definition of an effective temperature, with a thermodynamic meaning, implies that this quantity is independent of the chosen observable, which is not even verified in [13] where rheological and dielectric measurements do not lead to the same effective temperature. Is the effective temperature defined through a generalisation of FDR a relevant concept ? Does it depend on the chosen observable, as shown in the glass phase of Bouchaud's trap model [10], or not, as in simulations on a binary Lennard-Jones mixture [35] ? More experimental investigations are needed to understand these contradictory findings (see [36] for a brief review).

Dynamical heterogeneities are recognized as a general feature of slow dynamics encountered in supercooled liquids and glasses [37, 38, 39]. In supercooled liquids, deviations from the Einstein relation were explained by such dynamical heterogeneities [37]. Up to now, in models and simulations, deviations from FDR have been found in homogeneous glassy systems and interpreted as an effective temperature. Moreover, the effective temperature is defined as an ensemble-averaged quantity in experiments, models and simulations. Understanding how the concept of effective temperature interplays with such heterogeneities is an open question.

[1] L.F. Cugliandolo and J. Kurchan, *Phys. Rev. Lett.* **71**, 173 -176 (1993).
[2] L.F Cugliandolo, J. Kurchan, and L. Peliti, *Phys. Rev. E* **55**, 3898 - 3914 (1997).
[3] G. Parisi, *Phys. Rev. Lett.* **79**, 3660 - 3663 (1997).
[4] A. Barrat, *Phys. Rev. E* **57**, 3629 - 3632 (1998).
[5] M. Sellitto, *Acta Mechanica.* **4**, 135 - 138 (1998).
[6] E. Marinari, G. Parisi, F. Ricci-Tersenghi, and J.J. Ruiz-Lorenzo, *J. Phys. A : Math Gen.* **31**, 2611 - 2620 (1998).
[7] J.-L. Barrat and W. Kob, *Europhys. Lett.* **46**, 637 - 642 (1999).
[8] L. Berthier, J.-L. Barrat, and J. Kurchan, *Phys. Rev. E* **61**, 5464 - 5472 (2000).
[9] H.A. Makse and J. Kurchan, *Nature* **415**, 614 - 617 (2002).
[10] S. Fielding and P. Sollich, *Phys. Rev. Lett.* **88**, 050603-1 - 050603-4 (2002).
[11] T.S. Grigera and N.E. Israeloff, *Phys. Rev. Lett.* **83**, 5038 - 5041 (1999).
[12] L. Bellon, S. Ciliberto, and C. Laroche, *Europhys. Lett.* **53**, 511 - 517 (2001).
[13] L. Bellon and S. Ciliberto, *Physica D* **168 - 169** , 325 - 335 (2002).
[14] B. Abou and F. Gallet, *Phys. Rev. Lett.* **93**, 160603 1-4 (2004).
[15] D.R. Strachan, G.C. Kalur, and S.R. Raghavan, *Phys. Rev. E* **73**, 041509 1-5 (2006).
[16] S. Jabbari-Farouji, D. Mizuno, M. Atakhorrami, F.C. MacKintosh, C.F. Schmidt, E. Eiser, G.H. Wegdam, and D. Bonn, cond-mat/0511311 (2005).
[17] D. Hérisson and M. Ocio, *Phys. Rev. Lett.* **88**, 257202 - 257205 (2002).
[18] G. D'Anna, P. Mayor, A. Barrat, V. Loreto, and F. Nori, *Nature* **424**, 1909 - 912 (2003).
[19] R.P. Ojha, P.-A. Lemieux, P.K. Dixon, A.J. Liu, and D.J. Durian, *Nature* **427**, 521 - 523 (2004).
[20] T.G. Mason, K. Ganesan, J.H. van Zanten, D. Wirtz, and S.C. Kuo, *Phys. Rev. Lett.* **79**, 3282 - 3285 (1997).
[21] N. Pottier, *Physica A* **317**, 371 - 382 (2003); N. Pottier and A. Mauger, *Physica A* **332**, 15 - 28 (2004).
[22] N. Pottier *Physica A* **345**, 472 - 484 (2005);
[23] M. Kroon, W.L. Vos, and G.H. Wegdam, *Phys. Rev. E* **57**, 1962-1970 (1998).
[24] D.W. Thompson and J.T. Butterworth, *J. Colloid Interface Sci.* **151**, 236-243 (1992).
[25] D. Bonn, S. Tanaka, G.H. Wegdam, H. Kellay, and J. Meunier, *Europhys. Lett.* **45**, 52 - 57 1(1999).
[26] B. Abou, D. Bonn, and J. Meunier, *Phys. Rev. E* **64**, 021510 - 021513 (2001).
[27] B. Abou, D. Bonn, and J. Meunier, *J. Rheol.* **47**, 979 - 988 (2003).
[28] S. Hénon, G. Lenormand, A. Richert, and F. Gallet, *Biophys. J.* **76**, 1145 - 1151 (1999).
[29] J.-F. Berret, *Molecular gels*, Springer-Verlag, Weiss (Eds), 2005; cond-mat/0406681.
[30] R. Kubo, *Rep. Prog. Phys.* **29**, 255 - 284 (1966); R. Kubo, M. Toda, and N. Hashitsume, Statistical physics II : nonequilibrium statistical mechanics, Second edition, Springer-Verlag, Berlin, 1991.
[31] A. Knaebel, M. Bellour, J.-P. Munch, V. Viasnoff, F. Lequeux, and J.L. Harden, *Europhys. Lett.* **52**, 73 - 79 (2000).
[32] M. Bellour, A. Knaebel, J.L. Harden, F. Lequeux, and J.-P. Munch, *Phys. Rev. E* **67**, 031405 1-8 (2003).
[33] L.F. Cugliandolo, *Lecture notes, Les Houches* (2002); cond-mat/0210312.
[34] F. Ritort, *J. Phys. Chem. B* **109**, 6787 - 6792 (2005).
[35] L. Berthier and J.L. Barrat, *J. Chem. Phys.* **116**, 6228 - 6242 (2002).
[36] L. Cipelletti and L. Ramos, *Journal of Physics: Cond. Matt.* **17**, R253 - R285 (2005).
[37] S.F. Swallen, P.A. Bonvallet, R.J. McMahon, and M.D. Ediger, *Phys. Rev. Lett.* **90**, 015901 1-4 (2003).
[38] E.R. Weeks, J.C. Crocker, A.C. Levitt, A. Schofield, and D.A. Weitz, *Science* **287**, 627 - 631 (2000).
[39] A. Duri, P. Ballesta, L. Cipelletti, H. Bissig, and V. Trappe, *Fluctuation and noise Letter* **5**, L1 (2005).